OCEANOLOGY

Water Balance of the Caspian Sea in the Last Glacial Maximum and Pre-Industrial Conditions Based on the Experiments with the INMIO-CICE General Sea Circulation Model

P. A. Morozova[a,*], K. V. Ushakov[b,c], Academician V. A. Semenov[a,c,d], and E. M. Volodin[e]

Abstract—The INMIO-CICE hydrodynamic model of the Caspian Sea was used to calculate equilibrium river runoff and evaporation from the sea surface over a wide range of sea levels (from −85 to +50 m a.s.l.) for different climatic conditions: the Last Glacial Maximum (about 21 ka BP) and the pre-industrial climate (~1850). Data from the INMCM4.8 climate model were used as boundary conditions. It was found out that a river runoff of about 400 km³/yr was required in the Last Glacial Maximum to maintain the sea level at 35–50 m a.s.l. corresponding to the maximum values of the Khvalynian transgression. In the Last Glacial Maximum, evaporation from the sea surface decreased by 105–175 mm (12–22%), and a precipitation layer, according to the INMCM4.8 model, decreased by 50–70 mm (15–30%). These conditions caused the equilibrium runoff to decrease by about 10–20% compared to the pre-industrial conditions. Smaller absolute and relative changes corresponded to lower sea levels. The maximum evaporation decrease occurred at 5 m a.s.l.

INTRODUCTION

The level of the Caspian Sea (CS), a drainless water body, is an important indicator of climate changes in the entire drainage basin. It occupies a large part of the East European Plain and is characterized by major variations on different time scales: in the last century, the sea level changed by 4 m [4], and in the late Pleistocene, the amplitude could be more than 100 m [19]. The reasons for such fluctuations have not been definitely found. Due to the fact that the sea level is related to the river runoff and visible evaporation (the difference between evaporation and precipitation) from the sea surface, the level fluctuations are caused by variations in these hydrological balance components. The river runoff is related to the climatic conditions in the catchment area, and evaporation, in addition to climatic factors, also depends on the sea area [1]. Changes in watersheds and glacial runoff could also play an important role for the Late Glacial conditions [5, 8, 11].

The CS morphometric features are as follows: at a higher level, its area increases considerably northward; this process nonlinearly changes the ratio of water balance (WB) components in the lake. The use of global climate models to assess changes in the sea WB is subject to a number of limitations: low spatial resolution, use of simplified sea models, and current sea configuration in the PMIP4 paleoclimate experiments (Paleoclimate Modelling Intercomparison Project) [14].

The alternative approach is based on the use of a full hydrodynamic CS model with a high spatial resolution and with a free level, describing the sea dynamics and thermodynamics, including evaporation. Due to low temperatures in the Last Glacial Maximum (LGM) period and a large shallow water zone in the north under the CS transgression, ice distribution and duration of closed water periods greatly contributed to reducing the surface evaporation. Therefore, a detailed description of marine dynamic processes and heat−water exchange at the water−ice−atmosphere boundary makes it possible to clarify the amount of evaporation in comparison with the global climate models. Necessary values of the WB components can

[a] *Institute of Geography, Russian Academy of Sciences, Moscow, 119017 Russia*

[b] *Shirshov Institute of Oceanology, Russian Academy of Sciences, Moscow, 117997 Russia*

[c] *Water Problems Institute, Russian Academy of Sciences, Moscow, 117971 Russia*

[d] *A.M. Obukhov Institute of Atmospheric Physics, Russian Academy of Sciences, Moscow, 119017 Russia*

[e] *Marchuk Institute of Numerical Mathematics, Russian Academy of Sciences, Moscow, 119333 Russia*

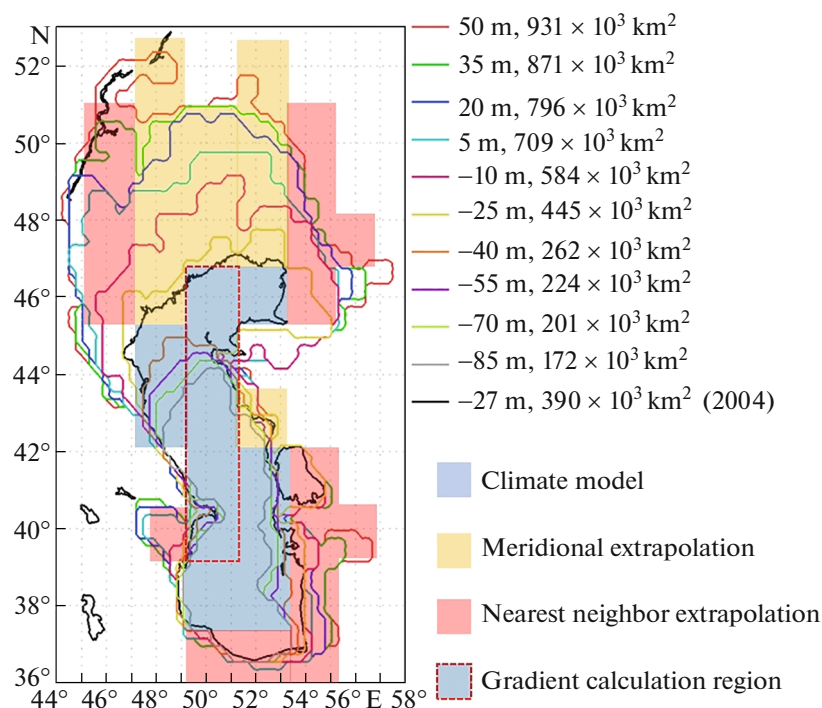**e-mail: morozova_polina@mail.ru*

Fig. 1. Coastline and CS area for considered levels in the INMIO-CICE model, as well as the CS calculation domain in the climate model and extrapolation zones when considering the transgression levels (color shading).

be estimated for different sea levels by setting the boundary climatic conditions in this regional CS model. This approach was applied in [6] to assess the CS WB components under the LGM conditions and in the pre-industrial (PI) climate for lake levels from −60 to −15 m above sea level (a.s.l.) relative to the current level of the World Ocean. The CS transgression was also considered in the range from −25 to +50 m a.s.l. in [11] for the LGM period and the Holocene Optimum.

This paper presents the modeled WB components of CS levels from −85 to +50 m a.s.l. covering the probable range of lake level changes in the period from the last glaciation to the present time [19]: the maximum level under the Khvalynian transgression could reach +48 m a.s.l., while the CS position under the regression was not clarified. The obtained estimates are important for the paleogeographic research, because no consensus on the nature, scale, and dating of transgression−regression events have been reached to date [2, 11, 19].

DATA AND METHODS

The CS WB component sensitivity was studied with the use of a coupled model of the ocean INMIO [13] and sea ice CICE [12] implemented in the CMF software environment [15]. This model is used in the weather forecasting and climate research [10, 17]. The model makes it possible to solve the equations of three-dimensional dynamics and thermodynamics of the ocean and sea ice cover. The calculations were carried out with the configuration adjusted for CS with a resolution of 0.27° in longitude and 0.2° in latitude, 28 vertical levels (step from 6 m near the surface to 125 m at the deep bottom), and a time step of 20 min.

The atmospheric boundary conditions used for INMIO-CICE included the experimental results of the INMCM4.8 climate model [18] to reproduce the LGM climate (LGM experiment, 21 ka BP) and the PI period climate (piControl experiment, about 1850), obtained under CMIP6 (Coupled Modeling Intercomparison Project) and PMIP4. The LGM experiment reproduces the maximum ice cover period in the last glaciation time; the boundary conditions and the first experimental results are reported in [14]. In the piControl experiment, boundary conditions, in particular, atmospheric composition are set for the end of the pre-industrial period. This is a control experiment to evaluate a sensitivity of the climate models to changing boundary conditions under CMIP6.

The boundary atmosphere conditions for the INMIO-CICE model include surface air temperature and humidity, precipitation, wind speed, and incoming long- and short-wave radiation fluxes. The extrapolation was carried out from the marine region of the climate model to the transgression region to model transgressive states for temperature and humidity fields, incoming long-wave radiation flux, demonstrating a noticeable deviation of average monthly isolines from the latitudinal distribution and repeating
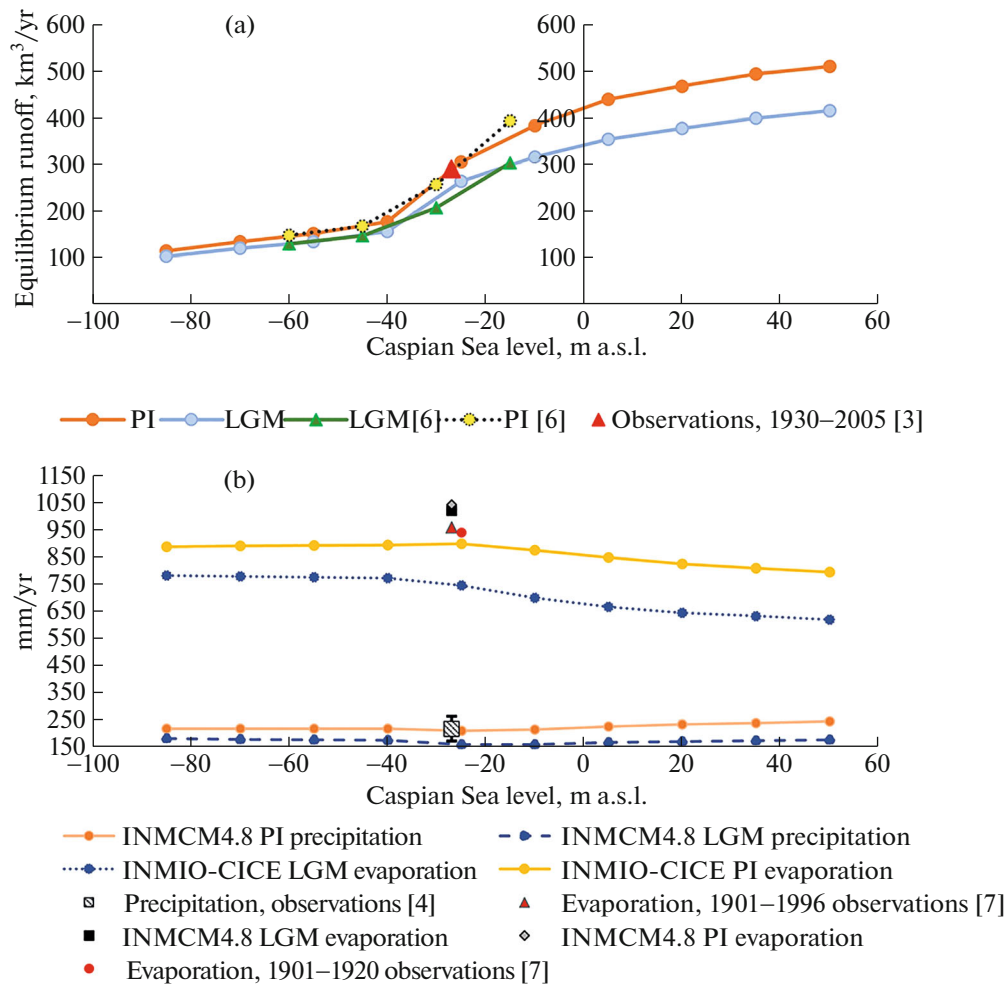
Fig. 2. WB components according to the modeling data at different CS levels, as well as according to the observations: (a) equilibrium runoff (km³/yr) (LGM [6] and PI [6], experimental results presented in [6]); (b) evaporation and precipitation layers averaged over the entire water area (mm/yr).

the coastline contours in the climate model. The extrapolation was carried out from the nearest sea cell to the south using the meridional gradient calculated by the least squares method over the central part of the climate model water area. As to the transgressive cells where this procedure is not applicable, simple extrapolation using the nearest neighbor method was performed (Fig. 1). This procedure is described in detail by [11].

The calculations were carried out for a series of CS levels: from −85 to +50 m a.s.l. with a step of 15 m (Fig. 1). A duration of each experiment was 50 years. First, a rough initial approximation for the average annual river runoff was set as a linear function of the water area (function coefficients were obtained in the preliminary experiments [6]). Then, the model was spun up for 5 years, and the average water imbalance was calculated for 6th−20th years of integration. The imbalance value was then used to adjust the river runoff. The resulting runoff value was considered as the

equilibrium and was used in further calculations. Finally, the average sea level over the water area was instantly returned to its original value, and the model was additionally spun up for 10 years; last 20 years of the experiment were used for further analysis.

RESULTS

Coupled calculations using the INMCM4.8 and INMIO-CICE models made it possible to estimate the CS WB components: Fig. 2 shows a river runoff volume (Fig. 2a) necessary to maintain the lake level at various marks (equilibrium flow), evaporation and precipitation averaged for the entire water area (Fig. 2b). A decrease in the evaporation layer as the level rises is due to the fact that the water reservoir's boundary under transgression shifts mainly northward where the temperature is lower and the ice coverage period is longer. Precipitation, on the contrary, increases, but this increase does not fully compensate for a decrease
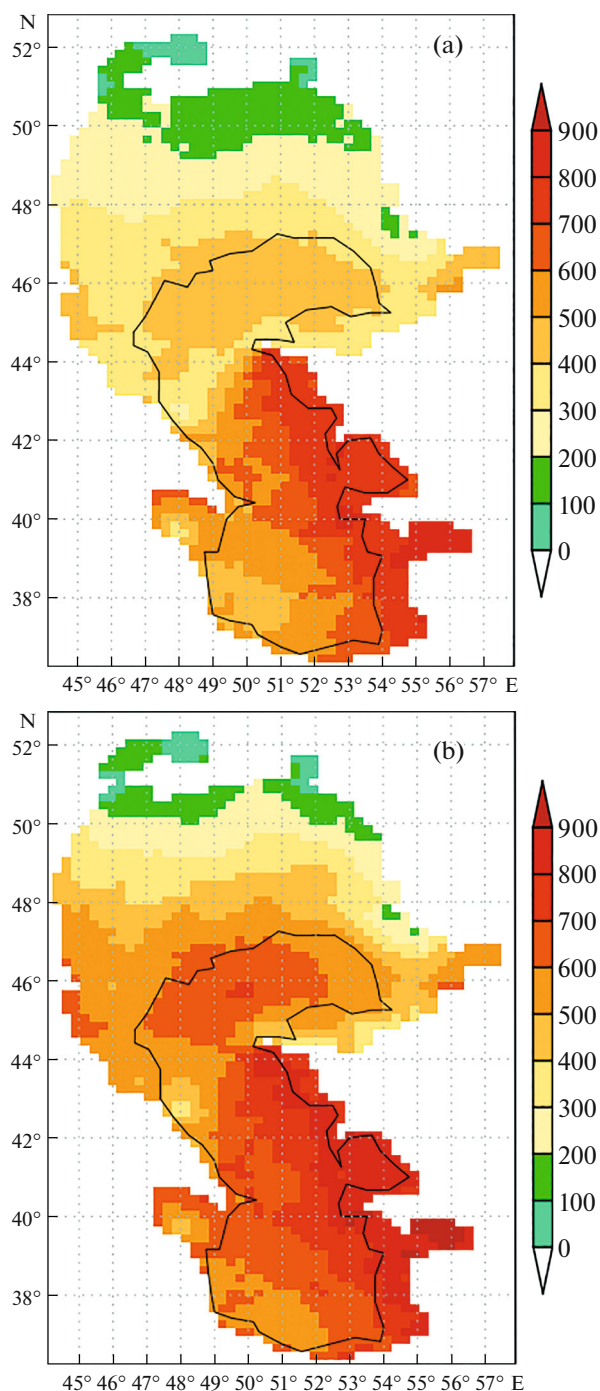
Fig. 3. Visible evaporation from the CS surface (mm/yr) for climatic conditions: (a) LGM; (b) PI period.

mate and 0.6 $(km^3/yr)/km^2 \times 10^3$ for LGM; and also a curve segment for levels of -25 m a.s.l. and above, when the lake area considerably increases at a higher level due to the shallow part in the north, and the gradient gradually decreases. In the range from -25 to -10 m a.s.l., it is about 0.55 $(km^3/yr)/km^2 \times 10^3$ for the PI climate and 0.4 $(km^3/yr)/km^2 \times 10^3$ for LGM. And in the range of $35-50$ m a.s.l., it is already about 0.25 $(km^3/yr)/km^2 \times 10^3$ for the PI climate and 0.15 $(km^3/yr)/km^2 \times 10^3$ for LGM. Levels of -60, -45, -30, and -15 m a.s.l. (Fig. 2a) were considered by [6]. The experiments were carried out in a similar way, but without the climate data extrapolation procedure which influenced the values obtained for the transgression conditions (-15 m a.s.l.). Despite a relatively wide range of levels from -60 to -15 m a.s.l., when compared with the curve obtained for the range from -85 to 50 m a.s.l., it is clear that a curve slope changes in the transgression conditions, but a series of experiments from -60 to -15 m a.s.l. do not cover it. Hence, linear extrapolation of the values obtained for the CS transgression conditions, close to the current ones, would be erroneous when estimating the lake balance at higher levels.

In the LGM period, evaporation and precipitation over the CS water area decreased substantially compared to the PI values (Fig. 3). This decrease led to variations in the equilibrium runoff values: for levels of above -25 m a.s.l., the LGM runoff was ~20% lower. The evaporation layer in the current CS boundaries is lower when calculated using the INMIO-CICE model than that based on the INMCM4.8 data (Fig. 2b). The values obtained with the help of the INMIO-CICE model seem to be more real, because they are slightly lower than those obtained from calculations based on the observations made in the twentieth century [7]. Similar values of the total river runoff observed in CS [3] and the model estimates confirm these data. The evaporation values obtained with the use of the INMCM4.8 climate model are higher than those obtained from the observation data; these data are indicative of the fact that evaporation was also overestimated by the climate model in colder conditions of the PI and LGM climate.

CONCLUSIONS

A series of experiments to reproduce the CS WB components for a wide range of possible levels: from -85 to $+50$ m a.s.l. for the LGM and PI climate conditions using the INMIO-CICE hydrodynamic model and the INMCM4.8 climate model make it possible to draw the following basic conclusions:

(1) the equilibrium runoff–CS level curve can be divided into three segments: "regression" (-40 m a.s.l. and below), when the lake area changes slightly under variations in its level, whereas the runoff volume gradient in terms of the area variations is maximum;

in evaporation, and the average visible evaporation also falls with increasing level (more than -25 m a.s.l.). Variations in the equilibrium runoff are proportional to those in the CS area, but the relationship is nonlinear for the entire range. It is possible to identify a curve segment for levels of -40 m a.s.l. and below, when the area changes slightly at variations in the level, the gradient is about 0.7 $(km^3/yr)/km^2 \times 10^3$ for the PI cli-

"transgression" (for levels of −25 m a.s.l. and above), when the lake area considerably increases with an increase in its level due to the shallow part in the north, whereas the gradient is lower than that of the regression conditions, and it gradually decreases with increasing area; and "close to current values" (from −40 to −25 m a.s.l.), when the lake area increases maximally in terms of a level increase meter, whereas the gradient values are relatively high and similar to the "regression" segment;

(2) in the LGM period, the evaporation layer decreased by 150 mm, while the precipitation layer decreased by 50 mm, on average. As a result, the equilibrium runoff also decreased: for levels of above −25 m a.s.l., the runoff was lower by ~20% compared to the PI experiment, and the runoff volume gradient in terms of the area variations also became lower in LGM;

(3) the river runoff in LGM calculated by [6, 16] makes it possible to exclude with a high degree of confidence a deep regression of the Caspian Sea in this period, because a river water volume (even according to the INMCM4.8 estimates which reproduced a maximum decrease in the Volga runoff (~50%) in the LGM period) was sufficient to maintain the Caspian Sea at a level of above −50 m a.s.l.;

(4) comparison of the obtained model estimates of the equilibrium runoff and paleo-reconstructions presented in [9], according to which the Volga runoff reached 420 km^3/yr in the Late Glacial period (18–13 ka BP), makes it possible to suggest a high probability of reaching the maximum levels of the Khvalynian transgression in this period.

FUNDING

CONFLICT OF INTEREST

The authors of this work declare that they have no conflicts of interest.

REFERENCES

1. K. Arpe, L. Bengtsson, G. S. Golitsyn, I. I. Mokhov, V. A. Semenov, and P. V. Sporyshev, Dokl. Earth Sci. **366** (2), 552−557 (1999).

2. R. N. Kurbanov, V. R. Belyaev, M. I. Svistunov, E. A. Butuzova, D. A. Solodovnikov, N. A. Taratunina, and T. A. Yanina, Izv. Ross. Akad. Nauk, Ser. Geogr. **87** (3), 403−419 (2023).

3. *River Mouths of the Caspian Region: History of Formation, Modern Hydrological-Morphological Processes and Dangerous Hydrological Phenomena,* Ed. by V. N. Mikhailov (GEOS, Moscow, 2013) [in Russian].

4. *Water Balance and Level Fluctuation of the Caspian Sea: Simulation and Prediction,* Ed. by E. S. Nesterov (Triada LTD, Moscow, 2016) [in Russian].

5. P. A. Morozova, Led Sneg, No. 1 (125), 113−124 (2014).

6. P. A. Morozova, K. V. Ushakov, V. A. Semenov, and E. M. Volodin, Water Resour. **48** (6), 823−830 (2021).

7. R. V. Nikolaeva and V. N. Bortnik, Vodn. Resur. **21** (4/5), 410−414 (1994).

8. A. V. Panin, A. Yu. Sidorchuk, and V. Yu. Ukraintsev, Water Resour. **48** (6), 877−886 (2021).

9. A. Yu. Sidorchuk, A. V. Panin, and V. Yu. Ukraintsev, Water Resour. **48** (6), 864−877 (2021).

10. R. Fadeev, K. Ushakov, M. Tolstykh, and R. Ibrayev, Russ. J. Num. Anal. Math. Modell. **33** (6), 333−340 (2018).

11. A. Gelfan, A. Panin, A. Kalugin, P. Morozova, V. Semenov, A. Sidorchuk, V. Ukraintsev, and K. Ushakov, Hydrol. Earth Syst. Sci. **28**, 241−259 (2024).

12. E. C. Hunke, W. H. Lipscomb, A. K. Turner, N. Jeffery, and S. Elliott, *CICE: the Los Alamos Sea Ice Model Documentation and Software User's Manual Version 5. Technical Report No. LA-CC-06-012.*

13. R. A. Ibrayev, R. N. Khabeev, and K. V. Ushakov, Izv. Atmos. Oceanic Phys. **48**, 37−46 (2012).

14. M. Kageyama, S. P. Harrison, M.-L. Kapsch, M. Lofverstrom, J. M. Lora, U. Mikolajewicz, S. Sherriff-Tadano, T. Vadsaria, A. Abe-Ouchi, N. Bouttes, D. Chandan, L. J. Gregoire, R. F. Ivanovic, K. Izumi, A. N. LeGrande, F. Lhardy, G. Lohmann, P. A. Morozova, R. Ohgaito, A. Paul, W. R. Peltier, C. J. Poulsen, A. Quiquet, D. M. Roche, X. Shi, J. E. Tierney, P. J. Valdes, E. Volodin, and J. Zhu, Clim. Past **17**, 1065−1089 (2021).

15. V. V. Kalmykov, R. A. Ibrayev, M. N. Kaurkin, and K. V. Ushakov, Geosci. Model Dev. **11** (10), 3983−3997 (2018).

16. A. Kalugin and P. Morozova, Climate **11** (2), 36 (2023).

17. K. V. Ushakov and R. A. Ibrayev, Russ. J. Earth. Sci. **18**, ES1004 (2018).

18. E. M. Volodin, E. V. Mortikov, S. V. Kostrykin, V. Y. Galin, V. N. Lykossov, A. S. Gritsun, N. A. Diansky, A. V. Gusev, N. G. Iakovlev, A. A. Shestakova, and S. V. Emelina, Russ. J. Num. Anal. M **33**, 367−374 (2018).

19. T. A. Yanina, V. Sorokin, Yu. Bezrodnykh, and B. Romanyuk, Quat. Int. **465** (Pt. A), 130−141 (2018).

Translated by E. Maslennikova